cmgh

CELLULAR AND MOLECULAR GASTROENTEROLOGY AND HEPATOLOGY

ORIGINAL RESEARCH

Crohn's Disease Fibroblasts Overproduce the Novel Protein KIAA1199 to Create Proinflammatory Hyaluronan Fragments

Artin Soroosh,[1] Sami Albeiroti,[2] Gail A. West,[1] Belinda Willard,[3] Claudio Fiocchi,[1] and Carol A. de la Motte[1]

[1]Department of Pathobiology, [3]Research Core Services, Lerner Research Institute, Cleveland Clinic Foundation, Cleveland, Ohio; [2]Department of Pathology and Laboratory Medicine, University of California Los Angeles, Los Angeles, California

SUMMARY

The novel protein KIAA1199 is overproduced by Crohn's disease mesenchymal cells in vivo and in vitro. KIAA1199 is important for generating proinflammatory and profibrotic hyaluronan fragments. Interleukin 6, overproduced by Crohn's disease cells, regulates deposition of KIAA1199 by fibroblasts.

BACKGROUND & AIMS: Crohn's Disease (CD) is a chronic inflammatory disease of the gastrointestinal tract. Fibrosis, a serious complication of CD, occurs when activated intestinal fibroblasts deposit excessive amounts of extracellular matrix (ECM) in affected areas. A major component of the ECM is high-molecular-weight hyaluronan (HA) that, when depolymerized to low-molecular-weight fragments, becomes proinflammatory and profibrotic. Mechanisms for HA degradation are incompletely understood, but the novel protein KIAA1199 recently was discovered to degrade HA. We hypothesized that KIAA1199 protein is increased in CD colon fibroblasts and generates HA fragments that foster inflammation and fibrosis.

METHODS: Fibroblasts were isolated from explants of surgically resected colon tissue from CD and non–inflammatory bowel disease control (ND) patients. Protein levels and tissue distribution of KIAA1199 were assessed by immunoblot and immunostaining, and functional HA degradation was measured biochemically.

RESULTS: Increased levels of KIAA1199 protein were produced and deposited in the ECM by cultured CD fibroblasts compared with controls. Treatment of fibroblasts with the proinflammatory cytokine interleukin (IL) 6 increased deposition of KIAA1199 in the ECM. CD fibroblasts also produce significantly higher levels of IL6 compared with controls, and antibody blockade of IL6 receptors in CD colon fibroblasts decreased the level of KIAA1199 protein in the ECM. Colon fibroblasts degrade HA, however, small interfering RNA silencing of KIAA1199 abrogated that ability.

CONCLUSIONS: CD fibroblasts produce increased levels of KIAA1199 primarily through an IL6-driven autocrine mechanism. This leads to excessive degradation of HA and the generation of proinflammatory HA fragments, which contributes to maintenance of gut inflammation and fibrosis. *(Cell Mol Gastroenterol Hepatol 2016;2:358–368; http://dx.doi.org/10.1016/j.jcmgh.2015.12.007)*

Keywords: Crohn's Disease; Fibrosis; Hyaluronan; KIAA1199.

Crohn's disease (CD) is a chronic inflammatory condition that may affect the whole gastrointestinal tract and lead to serious complications, among which are fibrosis and stricture formation.[1,2] During the development of intestinal fibrosis, activated fibroblasts and myofibroblasts proliferate and deposit extracellular matrix (ECM) components in the affected areas.[3,4] Prolonged fibrosis ultimately leads to stiffening and thickening of the bowel wall, eventually occluding the lumen and causing intestinal obstruction, frequently necessitating surgical intervention for relief.[5]

The intestinal ECM, similar to that of other tissues, is composed of a complex network of proteins and proteoglycans that surround all cells and function with both structural and signaling capacities.[6] A particular ECM component of interest to this study is the glycosaminoglycan hyaluronan (HA) because it is produced in large amounts and is implicated in both inflammation and fibrosis.[7–10]

HA is a linear polymer strictly composed of repeating disaccharide units of glucuronic acid and N-acetylglucosamine and is present in most organs of the human body.[11] At the cytosolic side of the cell surface, a family of enzymes called hyaluronan synthases creates HA polymers, which are immediately extruded out of the cell.[12,13] HA can exist in a range of sizes and the function of HA is determined by its molecular weight.[14] Large-molecular-weight HA is present in most tissues, including the

Abbreviations used in this paper: **CD, Crohn's disease; DAMP, damage-associated molecular pattern; ECM, extracellular matrix; FBS, fetal bovine serum; HA, hyaluronan; HBSS, Hank's balanced salt solution; HIF, human intestinal fibroblasts; HYAL, hyaluronidase; IBD, inflammatory bowel disease; IL, interleukin; IL6R, interleukin 6 receptor; LC-MS, liquid chromatography–mass spectrometry; ND, non–inflammatory bowel disease control; NF-κB, nuclear factor-κB; PAGE, polyacrylamide gel electrophoresis; PBST, phosphate-buffered saline with 0.1% Tween-20; SDS, sodium dodecyl sulfate; siRNA, small interfering RNA; TGF, transforming growth factor; TLR, Toll-like receptor; TNF, tumor necrosis factor.**

Most current article

2352-345X

http://dx.doi.org/10.1016/j.jcmgh.2015.12.007

intestine, and is a component of the ECM of healthy tissue. Large HA is important for organ structure and homeostasis, providing vital support for hydration, lubrication, stability, and flexibility. In addition, there is evidence suggesting that large HA is anti-inflammatory.[15–17] In contrast, low-molecular-weight HA fragments generally are associated with pathologic situations. Classified as a damage-associated molecular pattern (DAMP), fragmented HA is recognized by cell surface immune receptors, including CD44,[18,19] Toll-like receptor (TLR) 2,[17,20] and TLR4,[17,21,22] on multiple cell types. A pathophysiologically relevant outcome of these ligand-receptor interactions is immune cell activation and promotion of heightened inflammatory responses. Depending on the cell type, the HA fragment–cell interaction stimulates different actions, including the production of various proinflammatory cytokines, such as tumor necrosis factor-α (TNF-α), interleukin (IL) 1β, and IL6, and the activation of transcription factors (nuclear factor-κB [NF-κB], activator protein 1) that promote an immune response.[17,23,24]

The process of HA fragment generation in tissues is not well understood. The main pathway of HA degradation and turnover in the body involves the family of hyaluronidase (HYAL) 1 and 2 enzymes and the cell surface protein CD44.[25] In this accepted model, CD44 binds large HA onto the cell surface, which allows HYAL2 to cut it into smaller fragments. The fragmented HA then is internalized and transported to the lysosome, where the acid-active enzyme HYAL1 degrades it into oligosaccharides, which typically are recycled.[26] In a recent study investigating mechanisms of HA degradation, the novel protein KIAA1199 was discovered to play an unknown, but necessary, role in the HA degradation process.[27]

KIAA1199 was first discovered as an inner-ear protein whose genetic mutations were linked to nonsyndromic hearing loss.[28] KIAA1199's function in cancer metastasis has been investigated, and recent studies have linked it to migration, proliferation, and general survival of numerous types of tumor cells.[29–33] In addition, it was discovered that large HA could not be degraded by cells lacking KIAA1199,[27,34] which prompted us to evaluate its potential role in HA fragment generation, DAMP activity, and fibrogenesis.

In the present study, we used proteomic analysis of intestinal fibroblast–derived ECM and observed that CD cells produce much higher levels of KIAA1199 protein compared with non–inflammatory bowel disease (IBD) cells. We also found higher levels in the fibroblasts and the surrounding medium. In addition, we showed that intestinal fibroblasts do not degrade large HA in the absence of KIAA1199. Furthermore, we identified an IL6-dependent autocrine mechanism underlying dysregulated KIAA1199 production by CD fibroblasts. These results introduce a novel mechanism involved in CD pathogenesis by showing that KIAA1199 plays a key role in HA fragmentation in the intestine and thus contributes to intestinal inflammation and fibrosis.

Materials and Methods

All authors had access to the study data and reviewed and approved the final manuscript.

Cell Culture

Primary cells were isolated as previously described[35] from sample tissue derived from surgically resected colons of human Crohn's disease or non-IBD (control; ND) patients provided by the Department of Surgical Pathology at the Cleveland Clinic under an Institutional Review Board–approved protocol. After dissecting mucosal layer strips from the colon surface, they were put through a series of washes (dithiothreitol, D0632-10G; Sigma-Aldrich, St. Louis, MO; for 30 minutes, Hank's balanced salt solution [HBSS] with penicillin-streptomycin-fungizone, 17-745E; Lonza, Walkersville, MD; for 3 hours) before they were minced (2 $\times$ 2 mm) and placed on etched marks of petri dishes and air dried for 10 minutes. Fibroblast media (Dulbecco's modified Eagle medium with high glucose, 10% fetal bovine serum (FBS [10437-028; Gibco, Waltham, MA], 2.5% HEPES [17-745E; Lonza, Walkersville, MD], 2% L-glutamine, and 1% penicillin-streptomycin-fungizone) was added and the plates were incubated at 37°C in 5% CO_2. When fibroblasts grew out, the pieces were removed, and the fibroblasts were allowed to grow to confluence. Confluent stock cultures were split by routine trypsinization at a 1:2 ratio once a week. Fibroblasts were used between passages 5 and 15.

Isolation and Harvest of ECM

Fibroblasts were grown for 13 days to allow for sufficient ECM production for detection. To isolate and harvest ECM, cells first were washed with HBSS, then lysed with 0.05% Triton X-100 (T8532, Sigma-Aldrich) for 10 minutes at 37°C. The lysate was aspirated and the plate was washed with 0.025 N NH_4OH for 2 minutes at room temperature. The plate then was washed 4 times with HBSS with Ca^{2+} and Mg^{2+}. The plate was scraped in a buffer consisting of 3% sodium dodecyl sulfate (SDS), 80 mmol/L Tris, and 10% glycerol with freshly added protease inhibitor cocktail[36] (P8340; Sigma-Aldrich).

Proteomic Analysis of the Intestinal ECM

A 40-μL aliquot of each matrix sample isolated from CD or non-IBD human intestinal fibroblasts (HIF) was used for running the SDS–polyacrylamide gel electrophoresis (PAGE). The sample was boiled and a standard SDS-PAGE was run on a Bio-Rad Criterion 12.5% Tris-HCl gel with a constant voltage of 150 V. A Bio-Rad dual-color prestained Precision Plus Protein standard (161-0374; Bio-Rad, Hercules, CA) was run as the molecular weight marker. The gel was fixed for 30 minutes in 50% ethanol/10% acetic acid, transferred to a plastic dish, and stained in the dark with Sypro-ruby protein gel stain overnight. The next morning the dye was removed, the gel was

washed in Sypro destain (10% methanol/7% acetic acid) twice for approximately 30 minutes, and equilibrated into water (3 × 5 minutes). The gel was scanned using a Typhoon Trio Imager (GE Healthcare, Piscataway, NJ) at an excitation wavelength of 610/30 to visualize total the protein present in the gel. The gels then were washed in destain overnight and restained with Gel-Code blue.

For protein digestion, the bands were cut to minimize excess polyacrylamide and divided into a number of smaller pieces. The gel pieces were washed with water and dehydrated in acetonitrile. The bands then were reduced with dithiothreitol and alkylated with iodoacetamide before the in-gel digestion. All bands were treated with trypsin, by adding 5 μL of 10 ng/μL trypsin in 50 mmol/L ammonium bicarbonate and incubating overnight at room temperature to achieve complete digestion. The peptides that were formed were extracted from the polyacrylamide in 2 aliquots of 30 μL 50% acetonitrile with 5% formic acid. These extracts were combined and evaporated to less than 10 μL in Speedvac (Thermo Fisher Scientific, Waltham, MA) and then resuspended in 1% acetic acid to make up a final volume of approximately 30 μL for liquid chromatography–mass spectrometry (LC-MS) analysis.

The LC-MS system was a Finnigan LTQ-Orbitrap Elite hybrid mass spectrometer system interphased with a Dionex Ultimate 3000 high-performance liquid chromatography system (Thermo Fisher Scientific). The high-performance liquid chromatography column was a Dionex 15 cm × 75 μm internal diameter Acclaim Pepmap C18, 2 μm, 100 Å, reversed-phase, capillary chromatography column. Five microliters of the extract was injected and the peptides were eluted from the column by an acetonitrile/0.1% formic acid gradient at a flow rate of 0.25 μL/min and were introduced into the source of the mass spectrometer online.

The digest was analyzed using the data-dependent multitask capability of the instrument acquiring full scan mass spectra to determine peptide molecular weights, and tandem mass spectra (MS/MS) to determine amino acid sequence in successive instrument scans.

Protein identification was performed by analyzing all MS/MS spectra using the Mascot program (version 2.3.02; Matrix Science, Boston, MA), which was used to search both the bovine and human references. These searches were performed with a fragment ion mass tolerance of 0.8 daltons and parent ion tolerance of 10 parts per million. Carbamidomethyl of cysteine was specified as a fixed modification, and oxidation of methionine was specified as a variable modification. The relative abundance of proteins in these samples was determined by comparing the number of spectra, termed *spectral counts*, used to identify each protein. Normalization of spectral counts to the total number of spectra identified for each sample was performed before relative protein quantification. This approach takes into account the sample-to-sample variation that is obtained when performing replicate analyses of a sample.

Immunohistochemistry

For staining of human colon tissue sections, histochoice-fixed (H120, Amresco, Solon, OH) and paraffin-embedded blocks of colon tissue from CD and non-IBD patients were sectioned onto microscope slides and deparaffinized. The section was blocked in HBSS and 2% FBS for 1 hour at room temperature, then incubated overnight at 4°C with antibody for KIAA1199 (ab76849, 1:100; Abcam, Cambridge, MA) or biotinylated HA binding protein (385911, 1:100; Calbiochem, Billerica, MA) in HBSS with 2% FBS. Coverslips were washed 3 times with HBSS before incubation in a solution of fluorescent-tagged secondary antibody (1:1000; Life Technologies, Carlsbad, CA) in HBSS with 2% FBS for 1 hour at room temperature. A coverslip was mounted onto the colon section with Vectashield with 4′,6-diamidino-2-phenylindole mounting medium (H-1200; Vector Labs, Burlingame, CA). Cultured fibroblasts grown on glass coverslips for 13 days were washed twice with HBSS and fixed in ice-cold methanol for 10 minutes and air-dried. Staining was performed as described earlier. Images were obtained using a Leica DM upright microscope (Leica, Wetzlar, Germany), with the images taken using Image ProPlus acquisition software. The confocal micrographs were obtained using a Leica TCS SP5 II Confocal/Multi-Photon high-speed upright microscope with Acousto-Optical Beam Splitter and Leica confocal software (Leica) for acquisition. Images taken for morphometric immunohistochemistry were obtained at 20× magnification using a Leica Slide Scanner SCN400 (Leica) and semiquantitative analysis was conducted using Image ProPlus computer software (Media Cybernetics, Rockville, MD).

Immunoblot

Fibroblasts were grown for 13 days. To harvest whole-cell lysates, cells were first washed in ice-cold phosphate-buffered saline twice, lysed, and scraped in a lysis buffer that included the following: 50 mmol/L Tris-HCl (pH 7.6), 300 mmol/L NaCl, 0.5% NP-40, 1 mmol/L EDTA, and 10% glycerol with freshly added protease inhibitor cocktail.[37] The total protein of whole-cell and matrix lysates was measured via BCA assay (23225; Pierce, Waltham, MA). Proteins were separated via SDS-PAGE using precast Tris/glycine-based 4%–15% gradient gels (456-1084; Bio-Rad) run at 125 V for 1 hour. The separated proteins in the gel were transferred onto a polyvinylidene difluoride membrane using a semidry transfer apparatus (170-4156; Bio-Rad). After transfer, the membrane was blocked with 5% milk in phosphate-buffered saline with 0.1% Tween-20 (PBST). After blocking, membranes were incubated with primary antibody for KIAA1199 (21129-1-AP, 1:5000; Proteintech, Rosemont, IL) or glyceraldehyde-3-phosphate dehydrogenase (ab9485, 1:10,000; Abcam) at 4°C overnight. After multiple washes, the membrane was incubated with secondary antibody for rabbit (NA9340, 1:10,000; GE Healthcare, Piscataway, NJ) for 1 hour at room temperature. All membrane-washing steps were performed with PBST. Protein bands were visualized using ECL prime chemiluminescent development (RPN2232; GE Healthcare) and

detected by BioMax XAR scientific imaging film (BX810; Laboratory Products Sales, Inc, Rochester, NY). Differences in chemiluminescent signal intensity were quantified using the ImageScanner III with the ImageQuantTL v7.0 software package (29000605; GE Healthcare, Piscataway, NJ).

Cytokines

TNF-α (#300-01A), IL1β (#200-01B), and IL6 (#200-06) were purchased from Preprotech industries (Rocky Hill, NJ). IL8 was from R&D Systems (#208-IL, Minneapolis, MN). The cytokines were used to treat cells at the following concentrations: TNF-α at 100 U/mL, IL1β at 100 U/mL, IL6 at 20 ng/mL, and IL8 at 20 ng/mL.

For cytokine stimulation experiments, approximately 150,000 colon fibroblasts were plated into each well of a 6-well plate. After allowing 3 days of growth to achieve confluence, the media was replaced with fresh media and cytokines were added at the aforementioned concentrations. The media and cytokines would be replaced every 3 days for the next 9 days. On day 13, the extracellular matrix was collected for immunoblot analysis as previously described.

IL6 Enzyme-Linked Immunosorbent Assay

Fibroblasts were grown for 13 days, and the media samples were collected for IL6 analysis. The IL6 concentration was measured using an enzyme-linked immunosorbent assay purchased from BioLegend (430504, San Diego, CA) per the manufacturer's instructions. The experimental plate was incubated with capture antibody overnight at 4°C. The next day, the plate was blocked for 1 hour. Then, sample was added and incubated for 2 hours at room temperature. The plate then was incubated with detection antibody for 1 hour, then with avidin–horseradish-peroxidase solution for 30 minutes. Substrate solution was then added and incubated for 15 minutes in the dark. A stop solution of 2 N HCl was added after incubation with substrate solution. Washing with PBST occurred between each step.

IL6-Receptor Blocking

CD fibroblasts (~150,000) were grown for 3 days, to reach confluence, in wells of a 6-well plate. The media then was replaced with fresh fibroblast media, and IL6-receptor (IL6R) antibody (BMS135, 1 ug/mL; eBioscience, San Diego, CA), mouse IgG (I5381, 1 ug/mL; Sigma-Aldrich), or media alone was added to each well. Each day, for 10 days, fresh aliquots of IL6R antibody, mouse IgG, or media was added to the wells at the same concentration. At the end of the 10 days, matrix was collected using the method described earlier.

Hyaluronan Degradation Assay

KIAA1199 was silenced using electroporation with small interfering RNA (siRNA) previously used by Yoshida et al[27] (10620312; Invitrogen; 5′-AAACAUUGAAAUAUU CGCCAUGCUC-3′). Nonsilencing control siRNA, called *scramble siRNA* (12935-300; Invitrogen), was used as a negative control. Trypsinized fibroblasts (~300,000) were electroporated (VPI-1002; Lonza, Walkersville, MD) and plated on 10-mm wells of 6-well plates with fibroblast media and incubated at 37°C and 5% CO_2. After 1 day of growth, the media was replaced with modified fibroblast media, which contained only 1% FBS. The cells designated for HA treatment were given 2 ug/mL of highly purified, biosynthesized, 1000-kilodalton HA (HYA-1000kEF-1; Hyalose, Oklahoma City, OK). After 48 hours of incubation, the media samples were collected and the whole-cell lysates were harvested. The media then were treated with 0.25 mg/mL Proteinase K (03115852001; Roche Applied Sciences, Indianapolis, IN) at 60°C overnight to degrade protein.[38]

Carbohydrate gel electrophoresis was used to determine whether the 1000-kilodalton HA was degraded. Electrophoresis was run on a 0.5% agarose gel in Tris-acetate-EDTA. The wells of the gel were loaded with media samples with tracking dye run at 30 V for 30 minutes, and then at 60 V for 3.5 hours. After full separation of carbohydrates, the gel was submerged in 0.25% Stains All (E9379; Sigma-Aldrich) in 50% ethanol, covered, and placed on an orbital shaker overnight at room temperature. The gel then was destained slowly with 10% ethanol. HA bands in the gel were scanned and quantified using the scanning and densitometry software previously described.[38]

Statistical Analyses

Statistical difference between groups was evaluated where appropriate by the unpaired 2-tailed Student *t* test, and all error bars drawn indicate the SEM. Graphing was completed using GraphPad Prism version 4.0c (GraphPad Software, Inc, La Jolla, CA).

Results

Proteomic Analysis of HIF-Produced ECM

We initially investigated whether the ECM produced by HIF isolated from CD patients is quantitatively and qualitatively different from that of non-IBD patients, and a proteomic analysis approach was used. ECM was isolated from 3 distinct CD and 2 non-IBD control colonic HIFs and subjected to LC-MS analysis. Combined analysis of all the CD and control samples identified a total of 146 unique human proteins, with an average of 95 proteins per individual sample. Twenty-five of the most abundantly expressed proteins in each sample were selected for further analysis (Supplementary Tables 1 and 2).

Of the 25 most abundant proteins in control samples, 24 also were identified among the top 25 most highly expressed proteins in CD samples. Of these 24 shared proteins, 22 were present at nearly equivalent levels in control and CD samples (0.5- to 1.5-fold range). With respect to the other 2 proteins, fibronectin isoform 3 was overexpressed (>1.5-fold), and ADAMSTS1 was reduced (<0.5-fold) in CD ECM compared with ND. Interestingly, fibronectin isoform 3 is among the most highly expressed proteins present in all samples, yet its level is nearly doubled in CD compared with control samples. Conversely, of the 25 most highly

Table 1. KIAA1199 Is Uniquely Expressed in CD Fibroblast Matrix Only

Protein	Accession	Averaged counts
5'-nucleotidase isoform 2 preproprotein	325651886	0.7 ± 0.9
60S ribosomal protein L30	4506631	0.5 ± 0.5
Angiopoietin-related protein 2 precursor	6912236	0.7 ± 0.9
Annexin A1	4502101	0.6 ± 0.6
Laminin subunit α-5 precursor	21264602	3.8 ± 5.9
Laminin subunit γ-1 precursor	145309326	2.6 ± 3.7
Protein KIAA1199 precursor	**38638698**	**0.8 ± 0.5**
Protein-glutamine γ-glutamyltransferase 2 isoform a	39777597	1.8 ± 0.1
Secreted frizzled-related protein 1 precursor	56117838	1.2 ± 1.4
Serine protease 23 precursor	6005882	0.6 ± 0.6
Secreted Protein Acidic and Rich in Cysteine-related modular calcium-binding protein 2 isoform 1 precursor	24308277	1.3 ± 1.2

NOTE. List of proteins found exclusively in CD matrix as determined by mass spectrometry analysis. Two independent experiments using 2 ND cell lines and 3 CD cell lines are shown. Data are averaged spectral counts ± SD.

expressed proteins in the CD samples, only one is not included in the top expressed ECM proteins of control samples (ie, basement-membrane–specific heparan sulfate proteoglycan: <0.5-fold) (Supplementary Tables 3 and 4).

In addition, the results identified several proteins uniquely present in the CD matrix (Table 1). Importantly, one protein, KIAA1199, recently was found to be involved in HA fragmentation,[27] and HA is up-regulated in the tissue of IBD patients.[39] Individual sample spectral counts of KIAA1199 of these samples are part of the data presented above.

Fibrotic CD Colon Tissue Expresses Increased Levels of KIAA1199 Protein in the Submucosa

We previously reported the presence of high levels of HA in the expanded muscularis mucosae region of inflamed CD colon,[39] and that muscularis mucosae mesenchymal cells are a major source of HA.[19] Because degradation of HA can lead to production of fragments that have the ability to drive mesenchymal cell proliferation and migration,[40] we investigated whether KIAA1199 protein, which is involved in HA degradation,[27] is present in control or CD colon tissue. In addition, we investigated whether KIAA1199 exists in close proximity to its substrate, HA. Immunohistochemical analysis of fibrotic CD colon tissue and non-IBD control (ND) colon tissue was performed. Representative confocal micrographs showed that in control colon sections, KIAA1199 is present in the epithelium, some mononuclear leukocytes, and muscularis mucosae mesenchymal cells (Figure 1*A*). In fibrotic CD tissue greater levels of KIAA1199 are observed, which is especially pronounced in the expanded submucosal region of the fibrotic CD colon sections compared with controls (Figure 1*B*). Importantly, KIAA1199 is abundantly expressed near HA deposits in the inflamed and fibrotic colon (Figure 1*B*), thus placing the HA degrading protein in intimate proximity to its substrate. The morphometrically quantified level of KIAA1199 protein in human colons shows that CD colons have inherently higher levels of KIAA1199 in the muscularis mucosae region of the colon (Figure 1*C*).

Fibrotic CD-Derived Fibroblasts Produce Increased KIAA1199 Protein

Based on the observation of increased expression of KIAA1199 in and around CD mesenchymal cells in vivo (Figure 1), we further investigated the expression and production of KIAA1199 in cultured intestinal fibroblasts. Previous data have shown that KIAA1199 may be present intracellularly and extracellularly.[41] Fluorescence immunohistochemical staining of both ND and CD colon fibroblasts, grown for 13 days to allow mature matrix deposition, consistently showed greater KIAA1199 staining in the CD colon fibroblasts compared with that of control cells (Figure 2*A*). The pronounced striated appearance in the CD cultures suggested that KIAA1199 was largely expressed either on cell surfaces or in the ECM, and we proceeded to assess the distribution of KIAA1199 protein in whole-cell extracts, in the secreted compartment (culture supernatant), and ECM alone. Immunoblot analysis showed significantly increased KIAA1199 protein in the whole-cell lysates (Figure 2*B*) and secreted fractions (Figure 2*C*) of CD colon fibroblasts compared with controls. Evaluation of KIAA1199 messenger RNA levels showed no significant difference between CD and ND colons at 13 days (data not shown). Analyses of isolated ECM deposition both by Western blot (Figure 2*D*) and mass spectrometry (Figure 2*E*) showed that KIAA1199 protein level is increased in the ECM of CD colon fibroblasts compared with control cells. Importantly, KIAA1199 is highly expressed in the ECM of cells expressing increased collagen and fibronectin (Supplementary Table 3), proteins that are characteristic of fibrosis.

IL6 Selectively Promotes Increased Deposition of KIAA1199 in the ECM of CD Colon Fibroblasts

To understand why unstimulated CD fibroblasts produce higher levels of KIAA1199, we investigated whether cytokines known to be associated with IBD pathogenesis could modulate its production. We exposed replicate cultures of control fibroblasts to medium alone, or optimal stimulatory amounts of TNF-α, IL1β, IL6, or IL8. A fresh dose of cytokine was added every 3 days over the 10-day culture period. Among the cytokines tested, only IL6 induced the increase of KIAA1199 protein in the ECM of the stimulated control fibroblasts (Figure 3*A*). To determine whether IL6 could increase KIAA1199 in the already overexpressing CD fibroblasts, we stimulated them with IL6. A significant

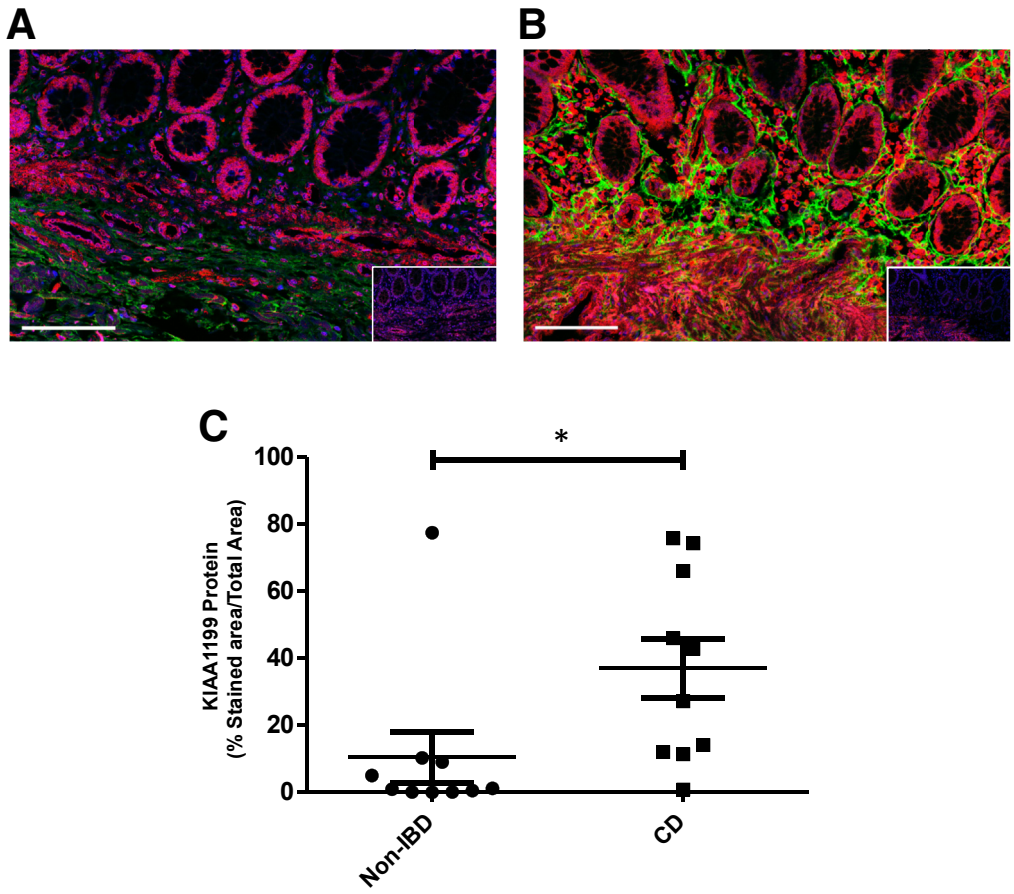

Figure 1. KIAA1199 is increased in the submucosal region of fibrotic CD colons. (*A*) A confocal image of a human colon tissue section from a non-IBD patient immunostained for KIAA1199 protein (red) and HA (green). (*B*) A confocal image of a human colon tissue section from a fibrotic CD patient immunostained for KIAA1199 protein (red) and HA (green). (*C*) Morphometric analyses of KIAA1199 protein in 10 CD and 10 control patient colon sections. Data points are the percentage of muscularis mucosae regions positive for KIAA1199 staining divided by the total muscularis mucosae areas analyzed. All data points have been normalized to the identical area on the nonspecifically stained serial section. All images were taken with a Leica TCS SP5 II Confocal/Multi-Photon high-speed upright microscope with Acousto-Optical Beam Splitter at 40× magnification, and acquisition was achieved with Leica confocal software. *Scale bars*: 100 μm. *Insets* are secondary antibody only (control) stained sections (*$P < .05$).

increase in KIAA1199 was observed, well beyond the basally overexpressed level (Figure 3*B*).

We next asked whether CD colon fibroblasts differentially secreted IL6 compared with control fibroblasts during the period of increased matrix deposition. Enzyme-linked immunosorbent assay analysis showed that supernatants of CD fibroblasts contained significantly higher levels of IL6 compared with supernatants of control cells (Figure 3*C*).

To determine whether the increased secretion of IL6 by CD fibroblasts contributes to the increase of KIAA1199 protein in the ECM, we performed an IL6R-blocking experiment. An anti-human IL6R-specific neutralizing antibody was added to the CD colon fibroblast cultures each day for the 10 days after reaching confluence. Immunoblot analyses showed that blocking IL6R on CD colon fibroblasts significantly decreased KIAA1199 levels in the ECM by approximately 50% (Figure 3*D*). Interestingly, the antibody treatment reduced KIAA1199 to the same protein levels typically expressed by control cells as seen in analyses in Figure 2*D*. These results suggest an IL6-dependent autocrine mechanism of KIAA1199 production by CD fibroblasts.

Intestinal Fibroblast-Derived KIAA1199 Promotes HA Degradation

A crucial question in our study was whether KIAA1199 produced by intestinal fibroblasts is involved in HA degradation as reported for skin fibroblasts.[27] To investigate this, we used a siRNA knockdown approach and measured degradation of purified, exogenously added, large-molecular-weight HA. Our results show that when KIAA1199 is silenced in fibroblasts, they no longer degrade exogenously added large-molecular-weight HA. This is true for CD and ND colon fibroblasts. Figure 4*A* shows that although cells transfected with scramble siRNA were able to degrade HA, those transfected with specific KIAA1199-directed siRNA were completely

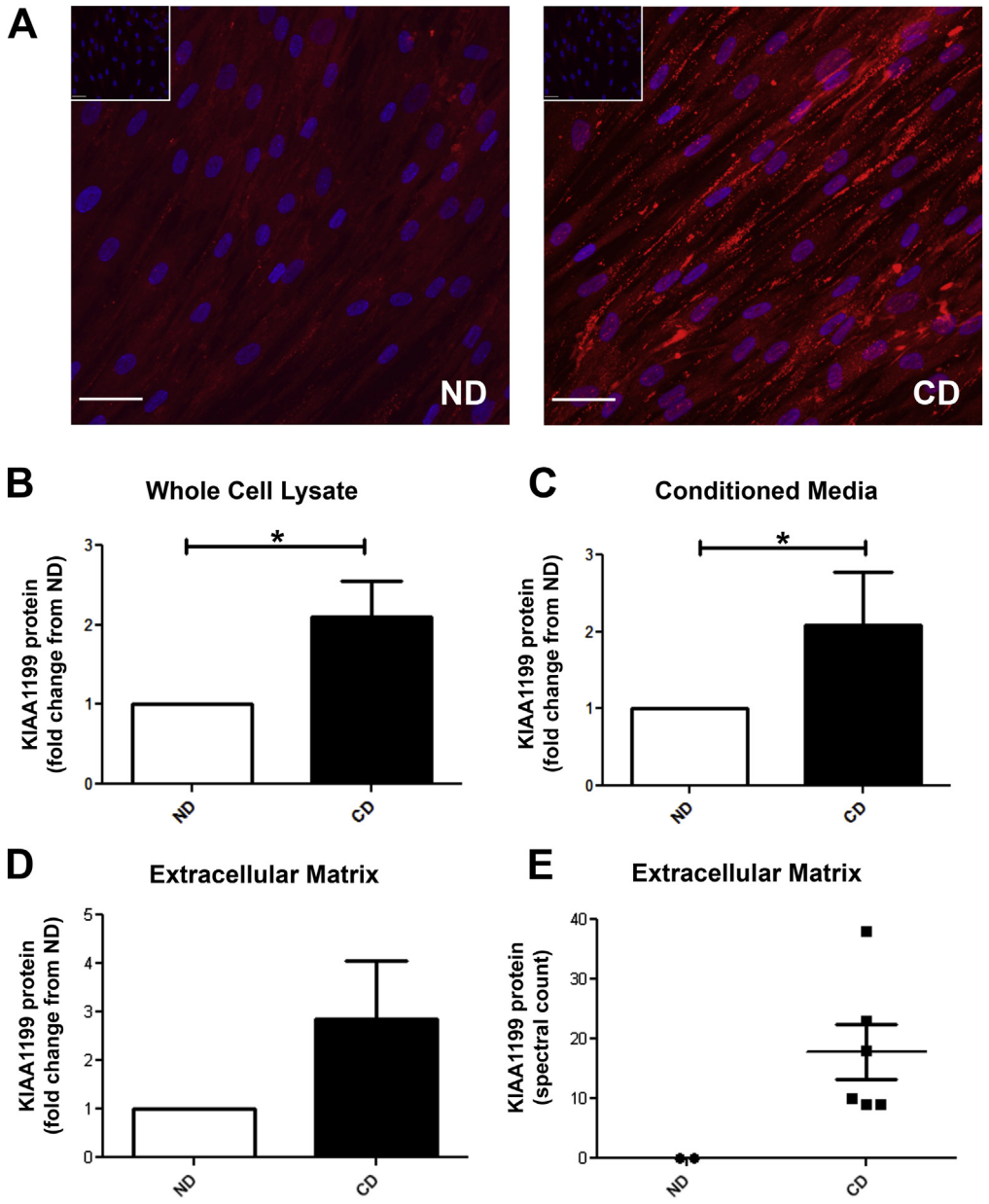

Figure 2. KIAA1199 is increased in fibroblasts derived from CD colons compared with fibroblasts from ND colons. (*A*) Fluorescent images of ND and CD colon fibroblasts grown for 13 days and immunostained for KIAA1199 (red) and 4′,6-diamidino-2-phenylindole (blue). *Insets* are secondary antibody (control) stained cells. *Scale bars*: 50 μm. Images were captured on a Leica DM upright microscope at 20× magnification with Image ProPlus acquisition software. (*B*) Average fold-change between densitometric measurements of immunoblots measuring KIAA1199 protein in CD and ND whole-cell lysate normalized to glyceraldehyde-3-phosphate dehydrogenase. Six independent experiments using 10 ND cell lines and 5 CD cell lines are shown. (*C*) Average fold-change between densitometric measurements from immunoblots of KIAA1199 protein in conditioned media from CD and ND fibroblasts grown for 13 days. Five independent experiments using 10 ND cell lines and 6 CD cell lines are shown. (*D*) Average fold-change of densitometric measurements from immunoblots comparing KIAA1199 protein in CD and ND ECM. Four independent experiments using 11 ND cell lines and 5 CD cell lines are shown. (*E*) Spectral counts from mass spectrometry measuring KIAA1199 protein in the ECM of CD and ND fibroblasts grown for 13 days. Two independent experiments using 2 ND lines and 3 CD lines are shown (*$P < .05$).

prevented from fragmenting HA. The representative carbohydrate sizing gel shows the dark staining band representing the exogenous HA alone (lane 1) and the lower-molecular-weight polydispersed band indicative of fragmentation of the exogenous HA added to mock silenced fibroblasts (lane 2). A single band at the original 1000-kilodalton size is evident in samples of HA incubated with fibroblasts after specifically silencing KIAA1199 (lane 3). Importantly, the gel shows high levels of released HA fragments in the scramble siRNA lane, implying that these cells do not clear the cleaved fragments by internalization. The inhibition of KIAA1199

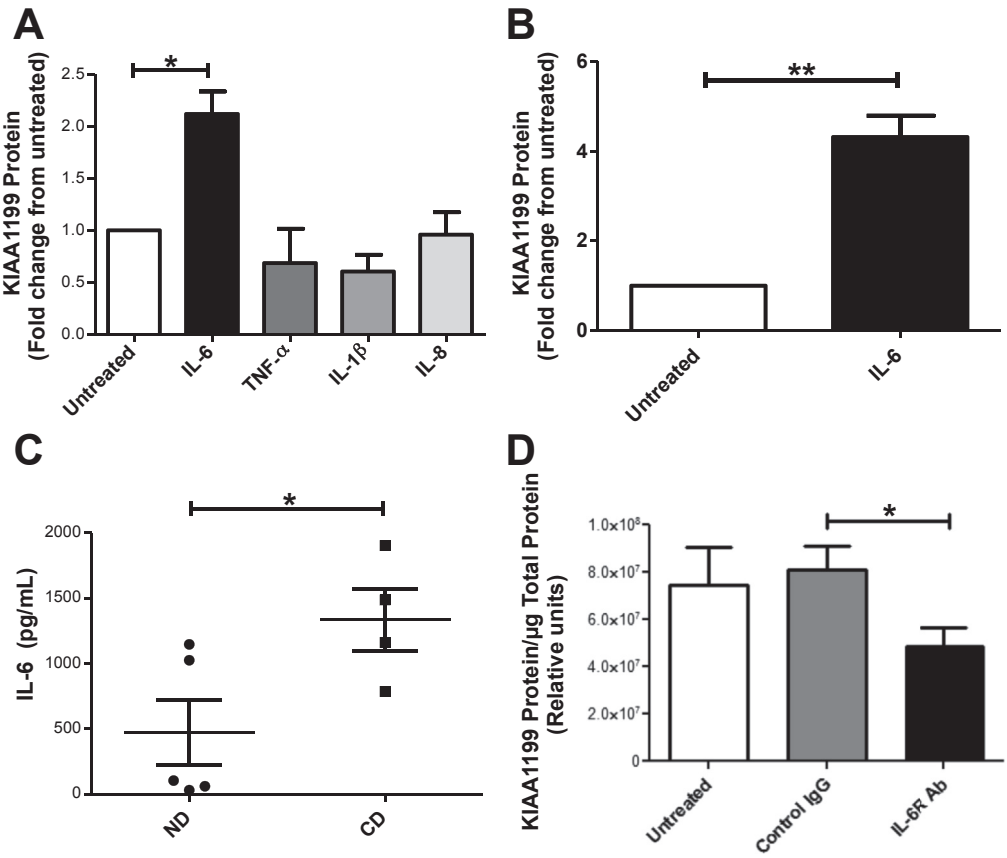

Figure 3. IL6 up-regulates KIAA1199 deposition into the ECM of colon fibroblasts. (*A*) Average fold-change between densitometric measurements of immunoblots measuring KIAA1199 protein in the ECM of cytokine-stimulated and unstimulated ND colon fibroblasts. Five independent experiments using 5 cell lines are shown. (*B*) Average fold-change between densitometric measurements of immunoblots measuring KIAA1199 protein in the ECM of IL6-stimulated and unstimulated CD colon fibroblasts. Four independent experiments using 4 cell lines are shown. (*C*) Comparison of IL6 protein levels in the conditioned media of CD and ND colon fibroblasts after 13 days of growth. Enzyme-linked immunosorbent assay determination of supernatants from 5 ND and 4 CD cell lines is shown. (*D*) Average densitometric measurements of immunoblots measuring KIAA1199 protein in the ECM of IL6R-blocking antibody–treated, mouse IgG-treated, and untreated CD colon fibroblasts. Five independent experiments using 5 cell lines are shown (*$P < .05$, **$P < .01$). Ab, antibody.

protein expression after siRNA treatment was confirmed by Western blot analysis (Figure 4*B*). Figure 4*C* shows the quantification of average differences in HA degradation capability between KIAA1199 silenced cells and mock siRNA-treated cells. Densitometric analyses of multiple assays showed a significant difference between the HA degradation capability of KIAA1199 knockdown cells and mock siRNA-transfected cells ($P < .001$).

Discussion

Small-size HA fragments are prototypical DAMPs capable of inducing proinflammatory cytokine production[23] and contributing to inflammation-driven fibrosis.[42] Our previous work has shown that the HA content is increased and differently organized in the intestine of active IBD patients, as well as in the colon of mice with experimental colitis.[43] This change in HA deposition is observed in the mucosal and submucosal layers, and is especially pronounced around muscularis mucosae cells.[39] Based on these observations, we investigated whether the expanded HA matrix could be fragmented into DAMPs that could exacerbate inflammation and fibrosis in IBD.

The mechanisms through which HA is cleaved from the ECM and fragments are generated are incompletely understood. Macrophages engaging in endocytosis using CD44, the major HA receptor, are thought to play an important role in clearing the inflammatory matrix and resolving tissue inflammation.[44] A similar mechanism previously was shown in skin fibroblasts,[45] but high levels of fragment generation seems unlikely in this process because macrophages and fibroblasts have the machinery to further degrade internalized HA to monosaccharides and disaccharides in their lysosomes.

Our group previously showed that human platelets carry 1 of 2 somatically active hyaluronidases, HYAL2, and platelets are capable of degrading a TNF-α–induced HA matrix in vitro. The HA fragments generated by platelets are released and capable of activating naive human peripheral blood monocytes to produce IL6 and IL8 proteins.[23] Further work has shown that platelets carry HYAL2 in α granules and must be activated to express the enzyme on their

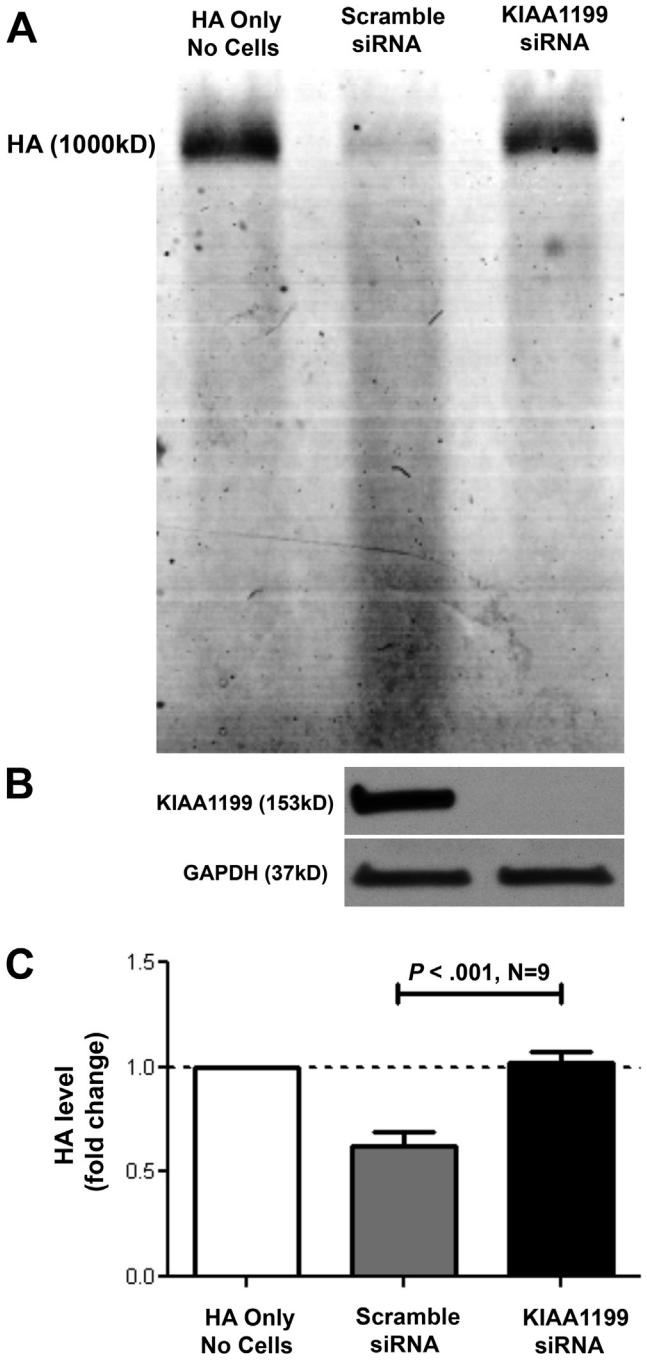

Figure 4. Colon fibroblasts cannot degrade exogenous HA in the absence of KIAA1199. (*A*) Representative carbohydrate-sizing electrophoresis gel showing hyaluronan after incubation with media only, mock siRNA-treated colon fibroblasts, and KIAA1199-knockdown colon fibroblasts. (*B*) Immunoblot image detecting KIAA1199 protein in mock siRNA and KIAA1199-knockdown colon fibroblasts. Glyceraldehyde-3-phosphate dehydrogenase (GAPDH) band included as loading control. (*C*) Average fold-change between densitometric measurements of carbohydrate-sizing electrophoresis gels measuring hyaluronan after incubation with media only, mock siRNA-treated colon fibroblasts, and KIAA1199-knockdown colon fibroblasts. Nine experiments using 9 cell lines are shown.

surfaces to cleave HA.[46] Interestingly, IBD patients are deficient in platelet HYAL2 protein expression.[46] Platelet cleavage of HA, however, does not seem like an efficient mechanism of HA fragment generation in solid extravascular tissues.

In this report, we show an alternate pathway for HA degradation, one in which mesenchymal cells of the intestine, being professional ECM-producing cells, could themselves possess intrinsic mechanisms regulating ECM turnover, specifically of HA. Recently, KIAA1199 was shown to participate in HA degradation, and our results have identified an overproduction of this protein specifically in intestinal fibroblasts from patients with active CD. In fact, intestinal fibroblasts functionally cleave exogenous HA, but cells lacking KIAA1199 protein lose the ability to degrade HA. We show that in the inflamed colon of CD patients there is increased HA deposition in the submucosal and muscularis mucosae areas of the intestinal wall. More importantly, fibroblasts isolated from these colons produce higher levels of KIAA1199 than control fibroblasts and this protein is both secreted and found bound to the matrix.

We found that IL6 induces non-IBD control fibroblasts to secrete increased levels of KIAA1199 in their matrix. Interestingly, proliferating fibroblasts, both control and CD-derived, produce comparable levels of IL6 (unpublished data). However, differential IL6 production was observed at confluence: CD fibroblasts continued to produce IL6 whereas control cell levels were greatly reduced, suggesting an important change in KIAA1199 production and regulation in the setting of chronic intestinal inflammation. Antibody blockade of the IL6 receptor in CD patient fibroblast cultures also reduces KIAA1199 protein levels, showing that IL6, but not other proinflammatory cytokines, is a selective key regulator of KIAA1199 production. This is important because IL6 production is greatly increased in CD tissues.[47] Therefore, high levels of KIAA1199 could be produced by autocrine IL6 as well as paracrine-supplied IL6 produced by inflammatory cells during active inflammation. This concept is supported by our finding that CD fibroblasts also deposit increased levels of KIAA1199 in response to exogenous IL6 stimulation. Furthermore, we have observed that IL6 containing lamina propria mononuclear cell supernatant fluids increase the deposition of KIAA1199 into the ECM of non-IBD colon fibroblasts (Soroosh, unpublished data).

IL6 is involved in fibrogenic responses, and increased production of KIAA1199 could represent a novel profibrotic pathway. Walia et al[48] have shown a regulatory relationship between IL6 and the profibrotic cytokine transforming growth factor-β (TGFβ). Other investigators[49] have reported a synergistic relationship between IL6 and TGFβ in kidney fibrosis and that IL6 stimulates increased production of collagen and various glycosaminoglycans in dermal fibroblasts.[50] Further studies have shown that fibrosis stemming from unresolved inflammation is strongly dependent on IL6. This cytokine was shown to mediate T-helper cell 1 activity, which promotes fibrosis after a prolonged inflammatory state, and IL6–deficient mice developed less fibrosis.[51]

Although the profibrotic role of IL6 has been shown to involve different pathways, induction of fibrosis by HA fragments generated through an IL6-stimulated production of KIAA1199 represents an entirely novel component of fibrogenic responses, and perhaps one directly relevant to IBD.

The ways that KIAA1199 could contribute to fibrosis still largely are unknown, but HA degradation is likely to be involved. Interestingly, HA fragments have been shown to stimulate production of IL6 by monocytes.[23] Furthermore, HA fragments up-regulate TGFβ, expression of tissue inhibitor of matrix metalloproteinase-1, and collagen,[52] all of which are related to fibrosis. Interestingly, a recent report showed that KIAA1199 promotes epithelial-to-mesenchymal transition and cell survival.[53] Furthermore, Shostak et al[53] provided evidence that KIAA1199 is regulated by NF-κB, a well-known proinflammatory and profibrotic transcription factor. Moreover, NF-κB is stimulated by HA fragment interaction with cell surface receptors such as CD44 and TLR4 on immune cells.[54] Thus, it seems reasonable to speculate that HA fragment-driven NF-κB signaling increases KIAA1199, which then fosters more HA fragment creation to drive the chronic inflammatory and fibrotic cycle seen in CD.

In all, our data indicate that KIAA1199 is involved in the CD-related pathologic process stimulated by HA fragments. Future studies will determine whether KIAA1199 production by intestinal fibroblasts mediates intestinal fibrosis through additional mechanisms.

References

1. Latella G, Di Gregorio J, Flati V, et al. Mechanisms of initiation and progression of intestinal fibrosis in IBD. Scand J Gastroenterol 2015;50:53–65.
2. Rieder F, Fiocchi C. Intestinal fibrosis in IBD—a dynamic, multifactorial process. Nat Rev Gastroenterol Hepatol 2009;6:228–235.
3. Simmons JG, Pucilowska JB, Keku TO, et al. IGF-1 and TGF-beta1 have distinct effects on phenotype and proliferation of intestinal fibroblasts. Am J Physiol Gastrointest Liver Physiol 2002;283:G809–G818.
4. Pucilowska JB, McNaughton KK, Mohapatra NK, et al. IGF-1 and procollage alpha1(I) are coexpressed in a subset of mesenchymal cells in active Crohn's disease. Am J Physiol Gastrointest Liver Physiol 2000;279:G1307–G1322.
5. Rieder F, Zimmermann EM, Remzi FH, et al. Crohn's disease complicated by strictures: a systematic review. Gut 2013;62:1072–1084.
6. Hay ED. Cell biology of extracellular matrix. New York, NY: Plenum Press, 1991.
7. Bollyky PL, Bogdani M, Bollyky JB, et al. The role of hyaluronan and the extracellular matrix in islet inflammation and immune regulation. Curr Diab Rep 2012;12:471–480.
8. Meran S, Thomas D, Stephens P, et al. Involvement of hyaluronan in regulation of fibroblast phenotype. J Biol Chem 2007;282:25687–25697.
9. Albeiroti S, Soroosh A, de la Motte CA. Hyaluronan's role in fibrosis: a pathogenic factor or a passive player? Biomed Research Int 2015;2015:79023.
10. Petrey AC, de la Motte CA. Hyaluronan, a crucial regulator of inflammation. Front Immunol 2014;5:101.
11. Fraser JR, Laurent TC, Laurent UB. Hyaluronan: its nature, distribution, functions and turnover. J Intern Med 1997;242:27–33.
12. Watanabe K, Yamaguchi Y. Molecular identification of a putative human hyaluronan synthase. J Biol Chem 1996;271:22945–22948.
13. Prehm P. Hyaluronate is synthesized at plasma membranes. Biochem J 1984;220:597–600.
14. Stern R, Asari AA, Sugahara KN. Hyaluronan fragments: an information-rich system. Eur J Cell Biol 2006;85:699–715.
15. Day AJ, de la Motte CA. Hyaluronan cross-linking: a protective mechanism in inflammation? Trends Immunol 2005;26:637–643.
16. Bollyky PL, Lord JD, Masewicz SA, et al. Cutting edge: high molecular weight hyaluronan promotes the suppressive effects of CD4+CD25+ regulatory T cells. J Immunol 2007;179:744–747.
17. Jiang D, Liang J, Fan J, et al. Regulation of lung injury and repair by Toll-like receptors and hyaluronan. Nat Med 2005;11:1173–1179.
18. Aruffo A, Stamenkovic I, Melnick M, et al. CD44 is the principal cell surface receptor for hyaluronate. Cell 1990;61:1303–1313.
19. de la Motte CA, Hascall VC, Calabro A, et al. Mononuclear leukocytes preferentially bind via CD44 to hyaluronan on human intestinal mucosal smooth muscle cells after virus infection or treatment with poly(I.C). J Biol Chem 1999;274:30747–30755.
20. Scheibner KA, Lutz MA, Boodoo S, et al. Hyaluronan fragments act as an endogenous danger signal by engaging TLR2. J Immunol 2006;177:1272–1281.
21. Taylor KR, Trowbridge JM, Rudisill JA, et al. Hyaluronan fragments stimulate endothelial recognition of injury through TLR4. J Biol Chem 2004;279:17079–17084.
22. Termeer C, Benedix F, Sleeman J, et al. Oligosaccharides of Hyaluronan activate dendritic cells via toll-like receptor 4. J Exp Med 2002;195:99–111.
23. de la Motte C, Nigro J, Vasanji A, et al. Platelet-derived hyaluronidase 2 cleaves hyaluronan into fragments that trigger monocyte-mediated production of proinflammatory cytokines. Am J Pathol 2009;174:2254–2264.
24. McKee CM, Lowenstein CJ, Horton MR, et al. Hyaluronan fragments induce nitric-oxide synthase in murine macrophages through a nuclear factor kappaB-dependent mechanism. J Biol Chem 1997;272:8013–8018.
25. Harada H, Takahashi M. CD44-dependent intracellular and extracellular catabolism of hyaluronic acid by hyaluronidase-1 and -2. J Biol Chem 2007;282:5597–5607.
26. Afify AM, Stern M, Guntenhöner M, et al. Purification and characterization of human serum hyaluronidase. Arch Biochem Biophys 1993;305:434–441.

27. Yoshida H, Nagaoka A, Kusaka-Kikushima A, et al. KIAA1199, a deafness gene of unknown function, is a new hyaluronan binding protein involved in hyaluronan depolymerization. Proc Natl Acad Sci U S A 2013; 110:5612–5617.
28. Abe S, Usami S, Nakamura Y. Mutations in the gene encoding KIAA1199 protein, an inner-ear protein expressed in Deiters' cells and the fibrocytes, as the cause of nonsyndromic hearing loss. J Hum Genet 2003; 48:564–570.
29. Matsuzaki S, Tanaka F, Mimori K, et al. Clinicopathologic significance of KIAA1199 in human gastric cancer. Ann Surg Oncol 2009;16:2042–2051.
30. Jami MS, Hou J, Liu M, et al. Functional proteomic analysis reveals the involvement of KIAA1199 in breast cancer growth, motility and invasiveness. BMC Cancer 2014;14:194.
31. Evensen NA, Kuscu C, Nguyen HL, et al. Unraveling the role of KIAA1199, a novel endoplasmic reticulum protein, in cancer cell migration. J Natl Cancer Inst 2013; 105:1402–1416.
32. Terashima M, Fujita Y, Togashi Y, et al. KIAA1199 interacts with glycogen phosphorylase kinase β-subunit (PHKB) to promote glycogen breakdown and cancer cell survival. Oncotarget 2014;5:7040–7050.
33. Xu J, Liu Y, Wang X, et al. Association between KIAA1199 overexpression and tumor invasion, TNM stage, and poor prognosis in colorectal cancer. Int J Clin Exp Pathol 2015;8:2909–2918.
34. Yoshida H, Nagaoka A, Nakamura S, et al. Murine homologue of the human KIAA1199 is implicated in hyaluronan binding and depolymerization. FEBS Open Bio 2013;3:352–356.
35. Strong SA, Pizarro TT, Klein JS, et al. Proinflammatory cytokines differentially modulate their own expression in human intestinal mucosal mesenchymal cells. Gastroenterology 1998;114:1244–1256.
36. Bonnefoy A, Legrand C. Proteolysis of subendothelial adhesive glycoproteins (fibronectin, thrombospondin, and von Willebrand factor) by plasmin, leukocyte cathepsin G, and elastase. Thromb Res 2000;98:323–332.
37. Hill DR, Rho HK, Kessler SP, et al. Human milk hyaluronan enhances innate defense of the intestinal epithelium. J Biol Chem 2013;288:29090–29104.
38. Lee HG, Cowman MK. An agarose gel electrophoretic method for analysis of hyaluronan molecular weight distribution. Anal Biochem 1994;219:278–287.
39. de la Motte CA, Hascall VC, Drazba J, et al. Mononuclear leukocytes bind to specific hyaluronan structures on colon mucosal smooth muscle cells treated with polyinosinic acid:polycytidylic acid: inter-alpha-trypsin inhibitor is crucial to structure and function. Am J Pathol 2003;163:121–133.
40. Tolg C, Telmer P, Turley E. Specific sizes of hyaluronan oligosaccharides stimulate fibroblast migration and excisional wound repair. PLoS One 2014;9:e88479.
41. Tiwari A, Schneider M, Fiorino A, et al. Early Insights to the function of KIAA1199, a markedly overexpressed protein in human colorectal tumors. PLoS One 2013; 8:e69473.
42. Ohkawara Y, Tamura G, Iwasaki T, et al. Activation and transforming growth factor-beta production in eosinophils by hyaluronan. Am J Respir Cell Mol Biol 2000; 23:444–451.
43. Kessler S, Rho H, West G, et al. Hyaluronan (HA) deposition precedes and promotes leukocyte recruitment in intestinal inflammation. Clin Transl Sci 2008;1:57–61.
44. Teder P, Vandivier RW, Jiang D, et al. Resolution of lung inflammation by CD44. Science 2002;296:155–158.
45. Tammi R, Agren UM, Tuhkanen AL, et al. Hyaluronan metabolism in skin. Prog Histochem Cytochem 1994; 29:1–81.
46. Albeiroti S, Ayasoufi K, Hill DR, et al. Platelet hyaluronidase-2: an enzyme that translocates to the surface upon activation to function in extracellular matrix degradation. Blood 2015;125:1460–1469.
47. Ito H. Anti-interleukin-6 therapy for Crohn's disease. Curr Pharm Des 2003;9:295–305.
48. Walia B, Wang L, Merlin D, et al. TGF-beta down-regulates IL-6 signaling in intestinal epithelial cells: critical role of SMAD-2. FASEB J 2003;17: 2130–2132.
49. Zhang XL, Topley N, Ito T, et al. Interleukin-6 regulation of transforming growth factor (TGF)-beta receptor compartmentalization and turnover enhances TGF-beta1 signaling. J Biol Chem 2005;280: 12239–12245.
50. Duncan MR, Berman B. Stimulation of collagen and glycosaminoglycan production in cultured human adult dermal fibroblasts by recombinant human interleukin 6. J Invest Dermatol 1991;97:686–692.
51. Fielding CA, Jones GW, McLoughlin RM, et al. Interleukin-6 signaling drives fibrosis in unresolved inflammation. Immunity 2014;40:40–50.
52. David-Raoudi M, Tranchepain F, Deschrevel B, et al. Differential effects of hyaluronan and its fragments on fibroblasts: relation to wound healing. Wound Repair Regen 2008;16:274–287.
53. Shostak K, Zhang X, Hubert P, et al. NF-$\kappa\beta$-induced KIAA1199 promotes survival through EGFR signaling. Nat Commun 2014;5:5232.
54. Noble PW, McKee CM, Cowman M, et al. Hyaluronan fragments activate an NF-kappa B/I-kappa B alpha autoregulatory loop in murine macrophages. J Exp Med 1996;183:2373–2378.

Received July 16, 2015. Accepted December 22, 2015.

Correspondence
Address correspondence to: Carol A. de la Motte, PhD, Lerner Research Institute of the Cleveland Clinic, NC22, 9500 Euclid Avenue, Cleveland, Ohio 44195. e-mail: delamoc@ccf.org; fax: (216) 636-0104.

Conflicts of interest
The authors disclose no conflicts.

Funding
Supported by the National Institutes of Health, Programs of Excellence in Glycosciences grants HL107147 (C.d.l.M.) and DK50984 (C.F.). Research reported here was supported by a NIH shared instrument grant. The Orbitrap Elite instrument was purchased via a National Institutes of Health shared instrument grant (1S10RR031537-01). Also supported by Nancy and Gerald Goldberg.

Supplementary Table 1. Twenty-Five Most Abundantly Expressed Proteins in ND Fibroblast Matrix With Comparison to CD Fibroblast Matrix as Determined by Mass Spectrometry Analysis

Protein	Accession	Averaged counts, CD matrix	Averaged counts, ND matrix	Ratio CD/ND
Keratin, type II cytoskeletal 1	119395750	61.9 ± 5.4	74.3 ± 4.6	0.8
Vimentin	62414289	55.8 ± 40.8	64.8 ± 56.0	0.9
Keratin, type II cytoskeletal 2 epidermal	47132620	49.3 ± 5.9	56.9 ± 7.2	0.9
EMILIN-1 precursor	5901944	62.6 ± 5.3	56.9 ± 2.7	1.1
Tenascin precursor	153946395	63.0 ± 21.8	56.6 ± 11.1	1.1
Keratin, type I cytoskeletal 10	195972866	45.0 ± 3.7	54.5 ± 1.3	0.8
Keratin, type I cytoskeletal 9	55956899	39.6 ± 0.8	52.6 ± 7.1	0.8
TGF-β–induced protein ig-h3 precursor	4507467	38.6 ± 7.6	40.3 ± 7.5	1.0
Fibronectin isoform 3 preproprotein	**16933542**	**54.0 ± 15.6**	**28.1 ± 4.4**	**1.9**
Keratin, type II cytoskeletal 5	119395754	21.1 ± 10.7	24.9 ± 7.9	0.8
Keratin, type II cytoskeletal 6A	5031839	19.3 ± 10.6	22.2 ± 13.6	0.9
Keratin, type I cytoskeletal 14	15431310	18.6 ± 4.5	19.3 ± 8.7	1.0
A disintegrin and metalloproteinase with thrombospondin motifs 1 preproprotein	**50845384**	**6.7 ± 1.1**	**17.0 ± 6.5**	**0.4**
Fibrillin-1 precursor	281485550	21.2 ± 7.8	15.4 ± 0.1	1.4
Serine protease HTRA1 precursor	4506141	20.2 ± 7.6	14.9 ± 3.0	1.4
Carboxypeptidase Z isoform 2 precursor	62388875	11.8 ± 3.1	13.8 ± 2.4	0.9
Desmoplakin isoform I	58530840	7.2 ± 6.9	11.4 ± 10.1	0.6
Insulin-like growth factor-binding protein 5 precursor	10834982	11.5 ± 1.1	11.2 ± 2.4	1.0
Keratin, type I cytoskeletal 16	24430192	12.4 ± 9.8	10.5 ± 8.9	1.2
40S ribosomal protein S3	15718687	5.0 ± 3.6	10.0 ± 10.5	0.5
Hornerin	57864582	8.8 ± 7.6	9.9 ± 10.7	0.9
Fibrillin-2 precursor	66346695	13.1 ± 5.2	9.7 ± 0.7	1.4
Actin, cytoplasmic 1	4501885	10.6 ± 2.7	9.4 ± 3.5	1.1
Coiled-coil domain-containing protein 80 precursor	41152074	10.6 ± 9.3	8.6 ± 5.9	1.2
Protein CYR61 precursor	31542331	8.6 ± 0.9	8.3 ± 1.3	1.0

NOTE. Two independent experiments using 2 ND cell lines and 3 CD cell lines are shown. Data are averaged spectral counts ± SD. Bolded/shaded entries are referred to in the Results section of this article.

Supplementary Table 2. Twenty-Five Most Abundantly Expressed Proteins in CD Fibroblast Matrix Compared With ND Fibroblast Matrix, as Determined by Mass Spectrometry Analysis

Protein	Accession	Averaged counts, CD matrix	Averaged counts, ND matrix	Ratio CD/ND
Tenascin precursor	153946395	63.0 ± 21.8	56.6 ± 11.1	1.1
EMILIN-1 precursor	5901944	62.6 ± 5.3	56.9 ± 2.7	1.1
Keratin, type II cytoskeletal 1	119395750	61.9 ± 5.4	74.3 ± 4.6	0.8
Vimentin	62414289	55.8 ± 40.8	64.8 ± 56.0	0.9
Fibronectin isoform 3 preproprotein	**16933542**	**54.0 ± 15.6**	**28.1 ± 4.4**	**1.9**
Keratin, type II cytoskeletal 2 epidermal	47132620	49.3 ± 5.9	56.9 ± 7.2	0.9
Keratin, type I cytoskeletal 10	195972866	45.0 ± 3.7	54.5 ± 1.3	0.8
Keratin, type I cytoskeletal 9	55956899	39.6 ± 0.8	52.6 ± 7.1	0.8
TGF-β–induced protein ig-h3 precursor	4507467	38.6 ± 7.6	40.3 ± 7.5	1.0
Fibrillin-1 precursor	281485550	21.2 ± 7.8	15.4 ± 0.1	1.4
Keratin, type II cytoskeletal 5	119395754	21.1 ± 10.7	24.9 ± 7.9	0.8
Serine protease HTRA1 precursor	4506141	20.2 ± 7.6	14.9 ± 3.0	1.4
Keratin, type II cytoskeletal 6A	5031839	19.3 ± 10.6	22.2 ± 13.6	0.9
Keratin, type I cytoskeletal 14	15431310	18.6 ± 4.5	19.3 ± 8.7	1.0
Fibrillin-2 precursor	66346695	13.1 ± 5.2	9.7 ± 0.7	1.4
Keratin, type I cytoskeletal 16	24430192	12.4 ± 9.8	10.5 ± 8.9	1.2
Carboxypeptidase Z isoform 2 precursor	62388875	11.8 ± 3.1	13.8 ± 2.4	0.9
Insulin-like growth factor-binding protein 5 precursor	10834982	11.5 ± 1.1	11.2 ± 2.4	1.0
Coiled-coil domain-containing protein 80 precursor	41152074	10.6 ± 9.3	8.6 ± 5.9	1.2
Actin, cytoplasmic 1	4501885	10.6 ± 2.7	9.4 ± 3.5	1.1
Hornerin	57864582	8.8 ± 7.6	9.9 ± 10.7	0.9
Protein CYR61 precursor	31542331	8.6 ± 0.9	8.3 ± 1.3	1.0
Basement membrane-specific heparin sulfate proteoglycan core protein precursor	**126012571**	**7.6 ± 4.3**	**0.8 ± 0.1**	**9.8**
Desmoplakin isoform I	58530840	7.2 ± 6.9	11.4 ± 10.1	0.6
A disintegrin and metalloproteinase with thrombospondin motifs 1 preproprotein	**50845384**	**6.7 ± 1.1**	**17.0 ± 6.5**	**0.4**

NOTE. Two independent experiments using 2 ND cell lines and 3 CD cell lines are shown. Data are averaged spectral counts ± SD. Bolded entries are referred to in the Results section of this article.

Supplementary Table 3. List of Detected Proteins That Are Increased More Than 1.5-fold in the CD Fibroblast Matrix Compared With ND Fibroblast Matrix, as Determined by Mass Spectrometry Analysis

Protein	Accession	Averaged counts, CD matrix	Averaged counts, ND matrix	Ratio CD/ND
Basement membrane-specific heparan sulfate proteoglycan core protein precursor	126012571	7.6 ± 4.3	0.8 ± 0.1	9.8
Myosin-Ic isoform b	124494247	0.9 ± 0.9	0.2 ± 0.3	4.5
Latent-TGF-β–binding protein 1 isoform LTBP-1L precursor	261337165	1.1 ± 1.2	0.3 ± 0.4	4.4
Collagen α-1(XIV) chain precursor	55743096	1.4 ± 1.3	0.3 ± 0.5	4.1
Extracellular sulfatase Sulf-2 isoform a precursor	29789100	2.2 ± 1.8	0.5 ± 0.8	4.0
Gremlin-2 precursor	71164892	1.4 ± 1.3	0.4 ± 0.6	3.3
Epidermal growth factor-like repeat and discoidin I-like domain-containing protein 3 precursor	31317224	2.3 ± 1.7	0.9 ± 0.2	2.6
Annexin A2 isoform 2	209862831	1.8 ± 1.6	0.8 ± 1.1	2.3
Integrin α-V isoform 2 precursor	223468595	1.7 ± 1.5	0.8 ± 1.1	2.2
Sulfide:quinone oxidoreductase, mitochondrial	10864011	0.9 ± 1.0	0.4 ± 0.6	2.2
Fibronectin isoform 3 preproprotein	16933542	54.0 ± 15.6	28.1 ± 4.4	1.9
Matrilin-2 isoform b precursor	62548862	0.9 ± 0.8	0.5 ± 0.7	1.9
Integrin β-5 precursor	20127446	0.7 ± 0.6	0.4 ± 0.6	1.8
Insulin-like growth factor- binding protein 3 isoform b precursor	62243068	1.4 ± 1.0	0.8 ± 1.2	1.7
Fibulin-2 isoform a precursor	51873053	5.8 ± 3.2	3.4 ± 0.3	1.7
Epidermal growth factor-containing fibulin-like extracellular matrix protein 2 precursor	320118911	1.0 ± 1.1	0.6 ± 0.9	1.6
ADAMTS-like protein 4 isoform 1 precursor	38016904	0.9 ± 0.8	0.6 ± 0.8	1.6
Fibroleukin precursor	5730075	1.6 ± 0.5	1.0 ± 0.3	1.6
Collagen α-1(VI) chain precursor	87196339	1.0 ± 0.1	0.7 ± 0.9	1.6
Protein Wnt-5b precursor	17402919	1.9 ± 1.7	1.3 ± 0.4	1.5

NOTE. Two independent experiments using 2 ND cell lines and 3 CD cell lines are shown. Data are averaged spectral counts ± SD.

Supplementary Table 4. List of Detected Proteins That Are Reduced More Than 50% in the CD Fibroblast Matrix Compared With ND Fibroblast Matrix, as Determined by Mass Spectrometry Analysis

Protein	Accession	Averaged counts, CD matrix	Averaged counts, ND matrix	Ratio CD/ND
40S ribosomal protein S10	66346695	0.6 ± 0.6	1.1 ± 1.6	0.5
40S ribosomal protein S3	4501885	5.0 ± 3.6	10.0 ± 10.5	0.5
Glyceraldehyde-3-phosphate dehydrogenase	41152074	0.5 ± 0.8	0.9 ± 0.5	0.5
Tissue factor pathway inhibitor 2 precursor	31542331	3.1 ± 0.6	6.9 ± 0.8	0.5
A disintegrin and metalloproteinase with thrombospondin motifs 5 preproprotein	29789100	1.8 ± 0.8	4.0 ± 1.1	0.4
Tenascin-X isoform1 precursor	71164892	1.5 ± 0.8	3.4 ± 3.4	0.4
40S ribosomal protein S5	31317224	1.0 ± 1.0	2.3 ± 2.2	0.4
Semaphorin-3B isoform 1 precursor	209862831	0.5 ± 0.5	1.2 ± 1.8	0.4
A disintegrin and metalloproteinase with thrombospondin motifs 1 preproprotein	223468595	6.7 ± 1.1	17.0 ± 6.5	0.4
Ras-related protein Ral-A precursor	10864011	0.4 ± 0.7	1.0 ± 0.2	0.4
Calpain-1 catalytic subunit	16933542	0.2 ± 0.3	0.6 ± 0.9	0.3
40S ribosomal protein S18	62548862	1.1 ± 1.4	3.6 ± 5.1	0.3
40S ribosomal protein S16	20127446	0.7 ± 0.6	2.3 ± 2.2	0.3
Plectin isoform1	62243068	1.7 ± 3.0	7.7 ± 10.8	0.2
40S ribosomal protein S4 X isoform	51873053	0.2 ± 0.4	1.2 ± 0.6	0.2
Desmoglein-1 preproprotein	320118911	0.2 ± 0.4	1.8 ± 1.8	0.1

NOTE. Two independent experiments using 2 ND cell lines and 3 CD cell lines are shown. Data are averaged spectral counts ± SD.